Development 136, 2791-2801 (2009) doi:10.1242/dev.031419

β1 integrins are required for the invasion of the caecum and proximal hindgut by enteric neural crest cells

Marie A. Breau*, Ahmed Dahmani, Florence Broders-Bondon, Jean-Paul Thiery† and Sylvie Dufour‡

Integrins are the major adhesive receptors for extracellular matrix and have various roles in development. To determine their role in cell migration, the gene encoding the β1 integrin subunit (*Itgb1*) was conditionally deleted in mouse neural crest cells just after their emigration from the neural tube. We previously identified a major defect in gut colonisation by conditional *Itgb1*-null enteric neural crest cells (ENCCs) resulting from their impaired migratory abilities and enhanced aggregation properties. Here, we show that the migration defect occurs primarily during the invasion of the caecum, when *Itgb1*-null ENCCs stop their normal progression before invading the caecum and proximal hindgut by becoming abnormally aggregated. We found that the caecum and proximal hindgut express high levels of fibronectin and tenascin-C, two well-known ligands of integrins. In vitro, tenascin-C and fibronectin have opposite effects on ENCCs, with tenascin-C decreasing migration and adhesion and fibronectin strongly promoting them. *Itgb1*-null ENCCs exhibited an enhanced response to the inhibitory effect of tenascin-C, whereas they were insensitive to the stimulatory effect of fibronectin. These findings suggest that β1 integrins are required to overcome the tenascin-C-mediated inhibition of migration within the caecum and proximal hindgut and to enhance fibronectin-dependent migration in these regions.

KEY WORDS: Enteric nervous system, Neural crest cell, Migration, Caecum, β1 integrins, Time-lapse imaging, Tenascin-C, Fibronectin, Mouse

INTRODUCTION

The development of the enteric nervous system (ENS) is a complex process whereby vagal neural crest cells colonise the whole intestine by migrating through the mesenchyme from its rostral to caudal extremities. During this colonisation, enteric neural crest cells (ENCCs) actively proliferate and differentiate into neurons and glial cells, which aggregate to form the ganglia of the mature ENS. The study of the dynamics of ENCC migration has revealed complex patterns of cell movements at the migratory front, which appear to be different within distinct portions of the gut. Chains of ENCCs form in the linear parts of the gut (the ileum and hindgut), whereas a higher number of isolated cells is found in the caecum and proximal hindgut (Young et al., 2004; Druckenbrod and Epstein, 2005; Druckenbrod and Epstein, 2007). These differences in the mode of ENCC migration suggest the existence of variations in the molecular mechanisms that drive ENCC progression along the rostrocaudal axis of the gut. This might be linked to the fact that ENCCs migrate through a non-homogenous extracellular environment, encountering successive gut regions that have distinct growth, signalling and differentiation states. For example, soluble factors that have been shown to regulate different aspects of ENCC biology in vitro are present locally along the rostrocaudal axis of the embryonic gut (Chalazonitis et al., 2004; Leibl et al., 1999; Woodward et al., 2000; Barlow et al., 2003; Young and Newgreen, 2001; Young et al., 2001; Natarajan et al., 2002; Anderson et al., 2007). In addition, several extracellular matrix (ECM) components are present in the gut wall during or after the gut colonisation by ENCCs, although variations in their expression patterns along the rostrocaudal axis of the gut have not been extensively analysed (Fujimoto et al., 1989; Newgreen and Hartley, 1995; Lefèbvre et al., 1999; Scherberich et al., 2004; Simon-Assmann et al., 1995; Bolcato-Bellemin et al., 2003).

Integrins, the major receptors for ECM, comprise a large family of 24 αβ heterodimers. The β1 integrins represent the largest subfamily, as the β1 chain can associate with 12 different α subunits. A number of integrins have been implicated in the control of cell migration. They are multifunctional and can also regulate cell proliferation, survival and differentiation, often through interaction with growth factors or cytokine receptors (Hynes, 2002; Larsen et al., 2006). In a previous study, the role played by β1 integrins in the colonisation of the gut by ENCCs was addressed by conditional deletion of the β1 integrin gene (*Itgb1*) in NCCs and their derivatives using the Ht-PA-Cre mouse line (Pietri et al., 2003). *Itgb1*-null ENCCs fail to completely colonise the gut, leading to an absence of ganglia in the descending colon, a defect resembling Hirschsprung's disease (HSCR) in humans. In addition, the absence of β1 integrins leads to the formation of abnormal ENCC aggregates in the gut wall of colonised regions and subsequently to extensive changes in the organisation of the postnatal ganglia network. *Itgb1*-null ENCCs survive, proliferate and differentiate normally within the gut. However, the migratory and adhesive properties of *Itgb1*-null ENCCs were impaired in a variety of gut explant cultures, suggesting that cell migration is the main process affected by the loss of β1 integrins in these cells (Breau et al., 2006).

Here, we used time-lapse imaging to analyse the migration of *Itgb1*-null ENCCs in the developing mouse gut. We showed that the migration defect of these cells primarily takes place during the invasion of the caecum and proximal hindgut, indicating that β1 integrins are required specifically for the colonisation of these regions. We observed high expression levels of two ECM components, tenascin-C (TNC) and fibronectin (FN), within the mesenchyme of these gut regions. We showed that TNC inhibits the adhesion and migration of ENCCs in vitro, with an enhanced effect

UMR144, CNRS–Institut Curie, 26 rue d'Ulm, 75248 Paris cedex 05, France.

*Present address: National Institute for Medical Research, Division of Developmental Neurobiology, Mill Hill, London NW7 1AA, UK
†Present address: IMCB A*STAR, 61 Biopolis Drive, Singapore 138673, Singapore
‡Author for correspondence (e-mail: sylvie.dufour@curie.fr)

Accepted 18 June 2009

on *Itgb1*-null ENCCs. By contrast, FN stimulated the adhesion and migration of control ENCCs, but not of *Itgb1*-null ENCCs. These findings strongly suggest that the combination of these two effects contributes to the region-specific nature of the migration defect in *Itgb1* mutant embryonic guts. Moreover, our data suggest that the coordinated and balanced effects of TNC and FN on wild-type ENCC adhesion and migration might play a role in the caecum and hindgut invasion in vivo.

MATERIALS AND METHODS

Animals

R26EYFP mice [referred to as YFP^{fl} mice (Srinivas et al., 2001)] were crossed with *Itgb1*-floxed (referred to here as $\beta1^{fl}$) mice (Potocnik et al., 2000) to obtain double homozygous $\beta1^{fl}/\beta1^{fl}$; YFP^{fl}/YFP^{fl} animals. *Ht-PA-Cre;* $\beta1^{+}/\beta1^{-}$ males were crossed with $\beta1^{fl}/\beta1^{fl}$; YFP^{fl}/YFP^{fl} females to disrupt the β1 integrin gene and express the *YFP* gene in ENCCs. *Tnc* mutant mice were provided by Prof. Melitta Schachner (Evers et al., 2002). The day of the vaginal plug was considered E0.5. Staging was further refined by examining embryo and gut morphologies and the position of the ENCC migratory front in controls (Kaufman, 1995; Young et al., 2001; Druckenbrod and Epstein, 2005).

Immunostaining

Immunostainings were carried out as described (Breau et al., 2006). The primary antibodies used are listed in Table 1. When needed, sections were pre-treated with chondroitinase ABC (Sigma) as described (Beauvais-Jouneau et al., 1997).

Gut explant cultures and time-lapse imaging

For ex-vivo time-lapse imaging, gut segments were placed in a drop of growth factor-reduced Matrigel (Becton Dickinson) on the bottom of a microdish containing DMEM/F12 (Invitrogen) with 5% horse serum (Babco). Explants were placed in a heated chamber under a Leica DMRBE videomicroscope equipped with a coolSNAP HQ camera (Roper Scientific), in a humid atmosphere of 5% CO_2/95% air. Up to six gut explants were imaged at the same time. YFP images were captured as described in the legends to Movies 1 and 3 in the supplementary material.

Two-dimensional (2-D) cultures of E12.5 midgut rings were performed on various mixtures of ECM components including vitronectin (VN, Sigma) at 10 μg/ml, FN (Sigma) at 10 μg/ml and TNC (Chemicon) at 20 μg/ml for 2 days in DMEM/F12 supplemented with insulin-transferrin-selenium (Gibco). Phase-contrast images were captured as described in the legend to Movie 5 in the supplementary material.

Individual ENCCs in ex-vivo cultures or on 2-D cultures were tracked using MetaMorph 7 software to determine their speed of locomotion and persistence of movement.

For graft experiments, segments of control and mutant distal midgut were grafted onto segments of $Tnc^{+/-}$ hindgut and cultured as described by Breau et al. (Breau et al., 2006) and in Fig. S3 in the supplementary material.

Gut dissociation and adhesion assay

Glass coverslips (18 mm) were incubated for 1 hour at 37°C with a diluted solution of the various ECM components (same concentrations as in the 2-D cultures of gut rings), and then with 3 mg/ml heat-inactivated BSA in PBS for 30 minutes. Coverslips were washed and deposited in 4-well plates. Midguts (without oesophagus and stomach regions) from E12 embryos were dissociated as described previously (Barlow et al., 2003). The cell suspension resulting from each dissociated midgut was divided in three equal volumes, which were plated onto the VN, VN+FN and VN+TNC substrata. The plates were incubated for 75 minutes at 37°C to allow cells to interact with the surfaces, washed with PBS to remove the non-adherent cells, fixed in 4% paraformaldehyde in PBS and stained for ENCC markers and with DAPI. Round and spread $NF160^{+}$ and $SOX10^{+}$ cells were counted with a Leica DM6000 microscope using a 40× objective. For each coverslip, 22-30 fields (up to 1300 cells) were analysed. Six control and five mutant guts were analysed in two independent experiments.

RESULTS

Dynamic behaviour of control and β1 integrin mutant ENCCs in the mouse caecum

Ht-PA-Cre/Ht-PA-Cre; $\beta1^{+}/\beta1^{-}$ mice were mated with $\beta1^{fl}/\beta1^{fl}$; YFP^{fl}/YFP^{fl} mice. The progeny obtained displayed *Ht-PA-Cre;* $\beta1^{+}/\beta1^{fl}$; YFP^{fl} and *Ht-PA-Cre;* $\beta1^{-}/\beta1^{fl}$; YFP^{fl} genotypes, which we refer to as controls and mutants, respectively. At birth, mutant animals had an aganglionic descending colon and an altered organisation of the ENS network (not shown), similar to those observed in the mutants studied previously [non-YFP (Breau et al., 2006)]. This indicated that Ht-PA-Cre-mediated recombination of the *Itgb1*-floxed allele in ENCCs is not modified by the presence of an additional *YFP*-floxed locus in these animals.

The timing of the stomach and midgut colonisation is not affected by the loss of β1 integrins (Breau et al., 2006) (see Fig. S1 in the supplementary material), but the colonisation of the caecum and hindgut is altered (Breau et al., 2006). To visualise the dynamic behaviour of ENCCs within the caecum and hindgut regions, we cultured gut or gut segments and followed ENCC migration by time-lapse imaging. At E11.5 (controls, n=8; mutants, n=8), we observed a small difference in the position of the migration fronts between mutants and controls. At the beginning of the time-lapse analysis, a few isolated ENCCs had entered the caecum region in controls, but not in mutant guts (Fig. 1A,B,F,G). In controls, a large number of isolated ENCCs detached from the population of cells at the base of the caecum. These cells were rapidly joined by more rostral ENCCs and formed small and dynamic groups of cells, either as aggregates or chains, that efficiently invaded the caecum body (Fig. 1A-E; see Movie 1 in the supplementary material). This pattern of migration

Table 1. Primary antibodies used for immunostaining

Antibody	Host	Source	Dilution
Neurofilament 160 kDa (NF160)	Mouse	DSHB, 2H3 clone	1/100
HuD	Mouse	J. A. Weston (Marusich et al., 1994), 16A11 clone	1/200
Brain fatty acid binding protein (B-FABP)	Rabbit	T. Müller (Kurtz et al., 1994)	1/500
SOX10	Guinea pig	M. Wegner (Maka et al., 2005)	1/1000
Aggrecan	Rabbit	Chemicon	1/50
Laminin 1	Rabbit	Sigma	1/100
Laminin α5	Rat	P. Simon-Assmann (Sorokin et al., 1997)	1/50
Collagen IV	Rabbit	Progen	1/100
Vitronectin	Rabbit	J. L. Duband (Neugebauer et al., 1991)	1/50
Tenascin-C	Rat	R and D Systems	1/100
Fibronectin	Rabbit	Sigma	1/100
Tenascin-W	Rabbit	Alexis Corporation	1/500

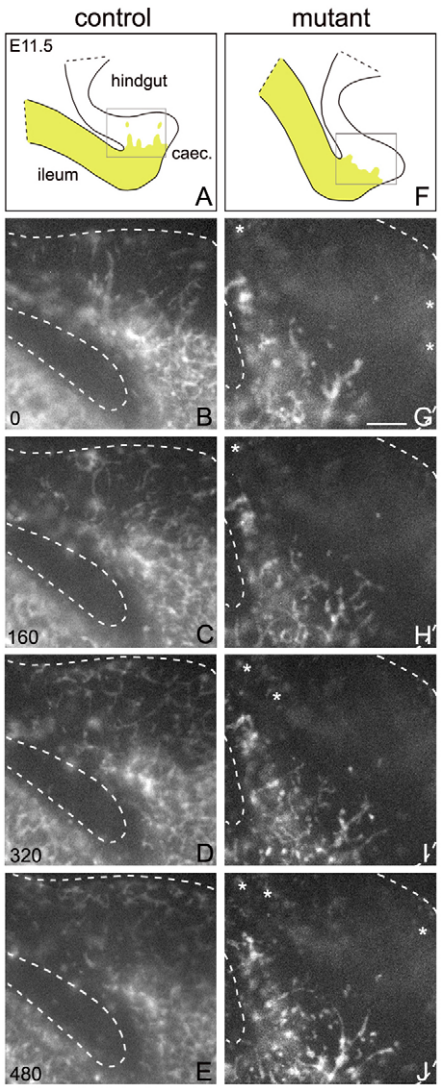

Fig. 1. Dynamic behaviour of leading control and mutant ENCCs in the caecum. (**A**,**F**) Schematics of control (A) and mutant (F) E11.5 mouse gut with regions colonised by YFP$^+$ ENCCs indicated in yellow. Boxes indicate regions imaged during the time-lapse sequence. Caec, caecum. (**B-E**,**G-J**) Illustration of the dynamic behaviour of control (B-E) and mutant (G-J) ENCCs (see also Movies 1 and 2 in the supplementary material). The limits of the gut tissue are indicated by dashed lines. The numbers indicate time in minutes. Asterisks indicate autofluorescent red blood cells. Scale bar: 50 μm.

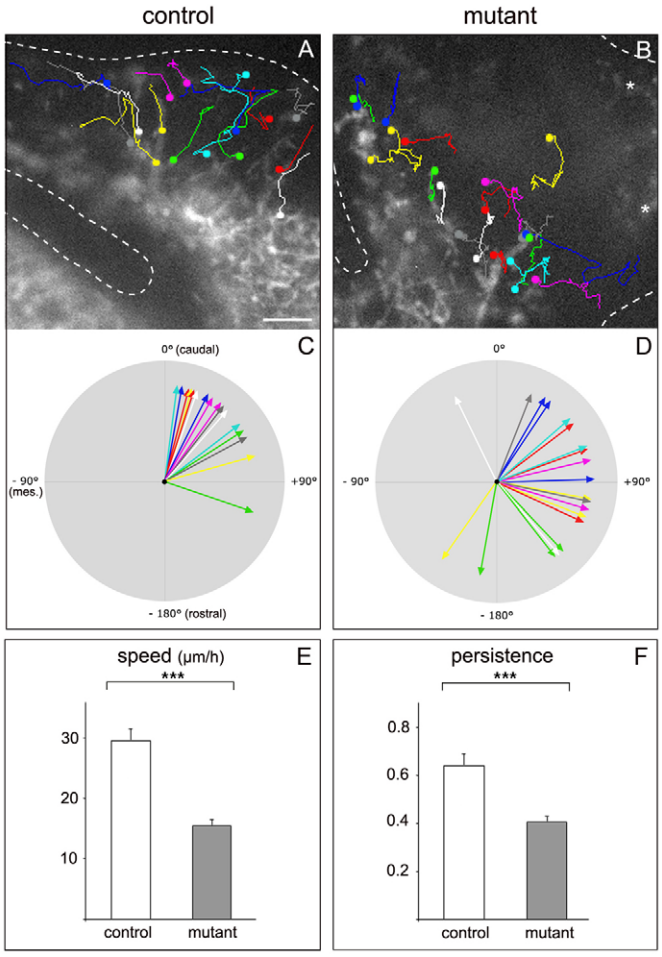

Fig. 2. Analysis of leading ENCC trajectories in the caecum. (**A**,**B**) Examples of individual trajectories of ENCCs at the migratory wavefront for control (A) and mutant (B) E11.5 mouse gut. The tracks overlay the first time-lapse image, with the initial positions of the cells indicated by circles. The limits of the gut tissue are indicated by dashed lines. Asterisks indicate autofluorescent red blood cells. (**C**,**D**) Mean directionality of tracked control (C) and mutant (D) ENCCs, evaluated by measuring the angle between the rostro-caudal axis of the gut and the straight line separating the initial and final positions of the cell. The colours of the arrows correspond to the colours of the trajectories in A and B. (**E**,**F**) Mean speed (E) and persistence (F) of leading ENCCs. The speed of each cell was calculated by dividing the total length of its trajectory by the time. Persistence was obtained by dividing the distance between its initial and final positions by the total distance covered by the cell. Control, n=16 cells; mutant, n=20. Error bars indicate s.e.m. ***P<0.001, Student's t-test. ENCCs tracked from another E11.5 mutant gut also exhibited a significant decrease in speed [10.3±1.25 μm/hour (P<0.005)] and persistence [0.49±0.05 (P<0.05)] and altered directionality (not shown) compared with the control. Mes, mesentery. Scale bar: 50 μm.

is consistent with previous observations (Druckenbrod and Epstein, 2005). By contrast, only very few ENCCs in the mutants were able to detach from strands located at the base of the caecum and move caudally. Once detached, these isolated cells remained round and immobile, and some of them even migrated rostrally towards the ileum (Fig. 1F-J; see Movie 2 in the supplementary material). Cell tracking was performed on two mutants and one control gut. The representation of individual cell trajectories at the E11.5 migratory front revealed the inability of the mutant ENCC population to enter the caecum region (Fig. 2B), whereas control ENCCs occupied the whole available space within the caecum (Fig. 2A). The speed of control ENCCs (29.5±1.25 μm/hour) is in agreement with previous observations (Druckenbrod and Epstein, 2005). The speed and persistence of leading cell movements were significantly reduced in the mutant (Fig. 2E,F). The directionality was also much more erratic in the mutant than the control, as ~50% of the leading cells migrated in the wrong (caudo-rostral) direction (Fig. 2C,D). Taken together, these observations indicate that the migratory capacity of *Itgb1*-null ENCCs is substantially reduced in the caecum.

Dynamic behaviour of control and β1 integrin mutant ENCCs in the proximal hindgut

We further analysed the dynamics of ENCC migration at later stages, during the proximal hindgut colonisation. At E12.5 in controls (*n*=7), ENCCs migrated in the hindgut by forming ramified chains with complex trajectories (Fig. 3B-G; see Movie 3 in the supplementary material). Some isolated pioneer cells were present at the leading front (Fig. 3B-D, red arrowheads) and were later joined by more rostral chains. The location of these intersections between chains and pioneer cells corresponded to nodes in the network that formed later, rostrally to the migratory front (Fig. 3E-G, red arrowheads). These findings are consistent with previous observations (Young et al., 2004). However, at this stage in mutants (*n*=7), ENCCs had not reached the proximal hindgut owing to their delayed invasion of the caecum (not shown). In time-lapse imaging performed on E13 mutant guts (*n*=2), we observed some mutant ENCCs beginning to colonise the proximal hindgut (Fig. 3H,I). Unlike controls, the migratory front in mutants was not organised into chains of cells. Rather, *Itgb1*-null ENCCs formed different types of aggregates in this region (Fig. 3I-N; see Movie 4 in the supplementary material). Most of these aggregates were large and dense and of variable shape and contour. Some cells were able to detach from these aggregates and migrate in all directions, either rostro-caudally or caudo-rostrally (Fig. 3J-L, green arrowheads), often forming new aggregates with other cells at new locations. Some of these aggregates formed thick 'chain-like' structures that were markedly more stable than control chains (Fig. 3L-N, blue arrowheads). In addition to these dynamic aggregates, smaller globular and static clusters of ENCCs were found more caudally (Fig. 3I, white arrowheads). However, the formation of these aggregates did not lead to efficient invasion of the proximal hindgut or to more caudal progression of the migration front. The behaviour of individual cells could not be followed in these groups (chains and aggregates) that were formed by both control and mutant ENCCs in this region and so we did not analyse the cell trajectories in these movies. Our results show that the migratory abilities of mutant ENCCs are still highly impaired in the proximal hindgut region, as they are unable to form invasive chains and instead form different types of aggregates.

ENCCs encounter a TNC- and FN-rich extracellular environment in the caecum and hindgut regions

The region-specific migratory defect of *Itgb1*-null ENCCs is not due to the timing of *Itgb1* deletion (Breau et al., 2006). Our results suggest that *Itgb1*-null ENCCs are unable to physically interact with their extracellular environment in the caecum and proximal hindgut. This could be due to the presence of a particular ECM component in these regions, with non-permissive or repulsive effects on *Itgb1*-null ENCC migration. We carefully examined the presence of various ECM components in E11.5 embryonic guts, including aggrecan, laminin α1 (LN1; LAMA1), laminin α5 (LNα5; LAMA5), collagen IV (ColIV), vitronectin (VN; VTN), FN, tenascin-W (TNW; tenascin-N – Mouse Genome Informatics) and TNC. Aggrecan, a protein sulphate proteoglycan that inhibits NCC adhesion and migration in other systems (Perris et al., 1996; Kerr and Newgreen, 1997), was not detected in E11.5 gut walls (not shown). LN1 and ColIV were present in the basal laminae around the gut epithelium, around blood vessels and at the base of the serosal layer (Fig. 4A,B,E,F). LNα5 was present in the basal laminae of the epithelium and in the serosal layer, but not around blood vessels (Fig. 4C,D). VN was found around most of the cells of the gut wall (Fig. 4G,H). By contrast, TNW was expressed at

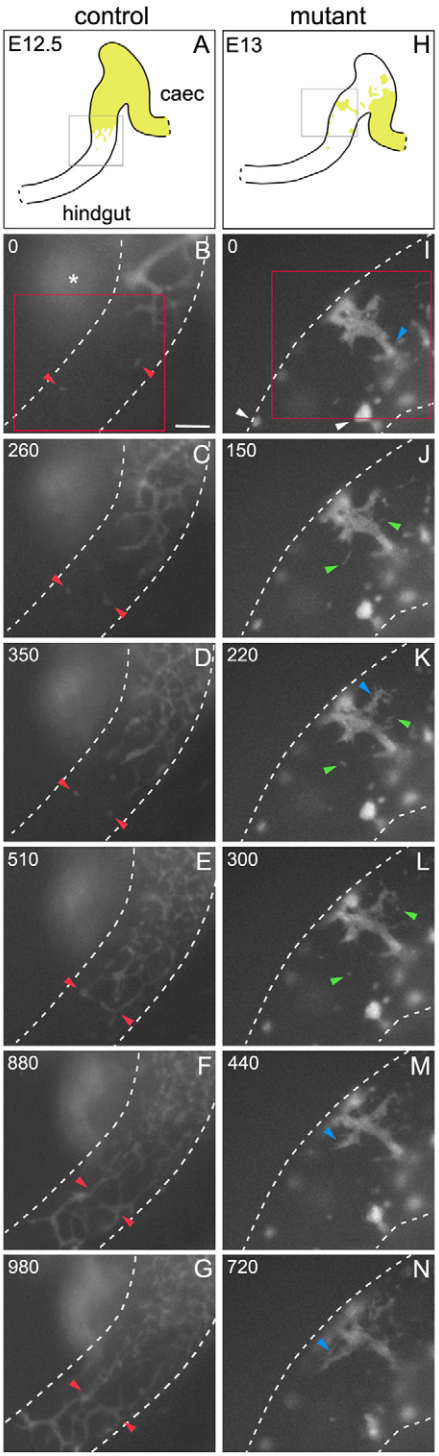

Fig. 3. Dynamic behaviour of leading control and mutant ENCCs in the proximal hindgut. (**A**,**H**) Schematics of control (A) and mutant (H) E12.5/13 mouse gut segments containing the distal ileum, caecum and hindgut, with the regions colonised by YFP$^+$ ENCCs indicated in yellow. Boxes indicate the regions imaged during the time-lapse sequence. (**B-G**,**I-N**) Illustration of the dynamic behaviour of control (B-G) and mutant (I-N) ENCCs. Red boxes in B and I indicate the regions shown in Movies 3 and 4 in the supplementary material, respectively. The numbers indicate time in minutes. The asterisk in B indicates a region of colonised ileum located in another focal plane. See text for comments on the arrowheads. Scale bar: 200 μm.

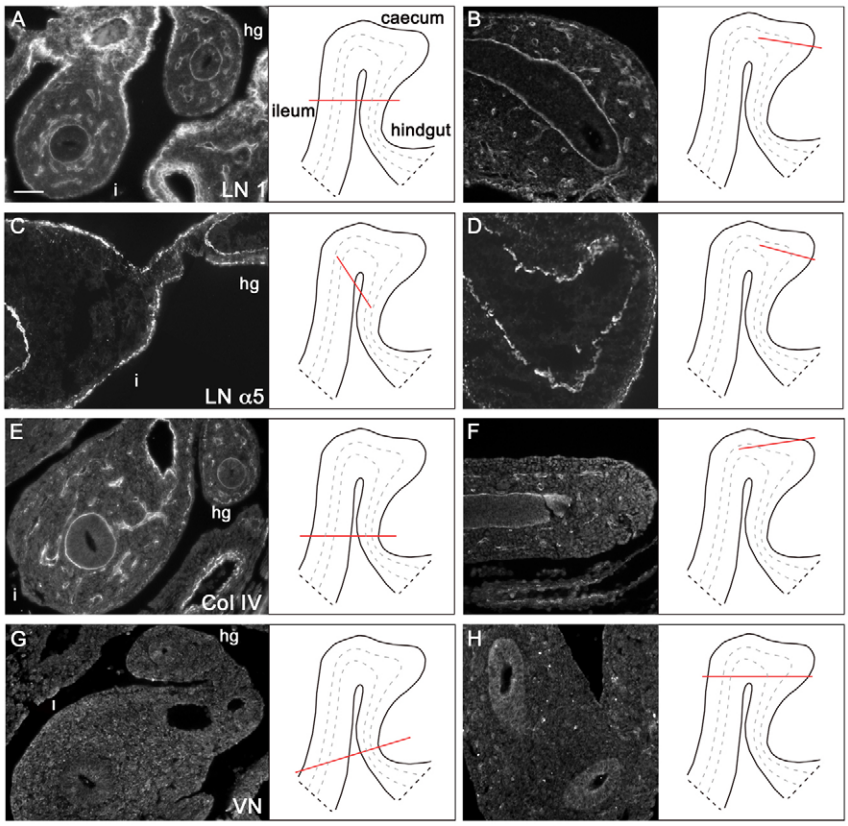

Fig. 4. Expression patterns of LN1, LNα5, ColIV and VN in the E11.5 gut. Immunostaining for LN1 (**A**,**B**), LNα5 (**C**,**D**), ColIV (**E**,**F**) and VN (**G**,**H**) on control E11.5 mouse gut sections. Accompanying schematics show the plane of section (red line), with the epithelium indicated by dashed lines. i, ileum; hg, hindgut. Scale bar: 50 μm.

low levels by just a few, isolated cells of the gut wall (not shown). The expression patterns of these ECM components were similar in all of the regions analysed along the rostrocaudal axis of the gut, encompassing the ileum, caecum and hindgut (Fig. 4). However, the expression patterns of FN and TNC were markedly different between gut regions. They were abundant in the caecum and hindgut mesenchymal layer, but present only at very low levels in the wall of the ileum (Fig. 5A-D). FN and TNC were organised into distinct fibrillar networks in the intercellular spaces of the mesenchyme (Fig. 5E-G). They were also found in the mesenteric region, and near the mesentery in the ileum (Fig. 5A,C), although they did not appear to be in direct contact with ENCCs in this region (not shown). Because chondroitin sulphate proteoglycans mask epitopes from other ECM components, we determined whether the presence of some of these glycoproteins could mask TNC and FN epitopes in the ileum. A pre-treatment with chondroitinase did not affect the expression pattern of TNC and FN (not shown), confirming the existence of the gradient of these

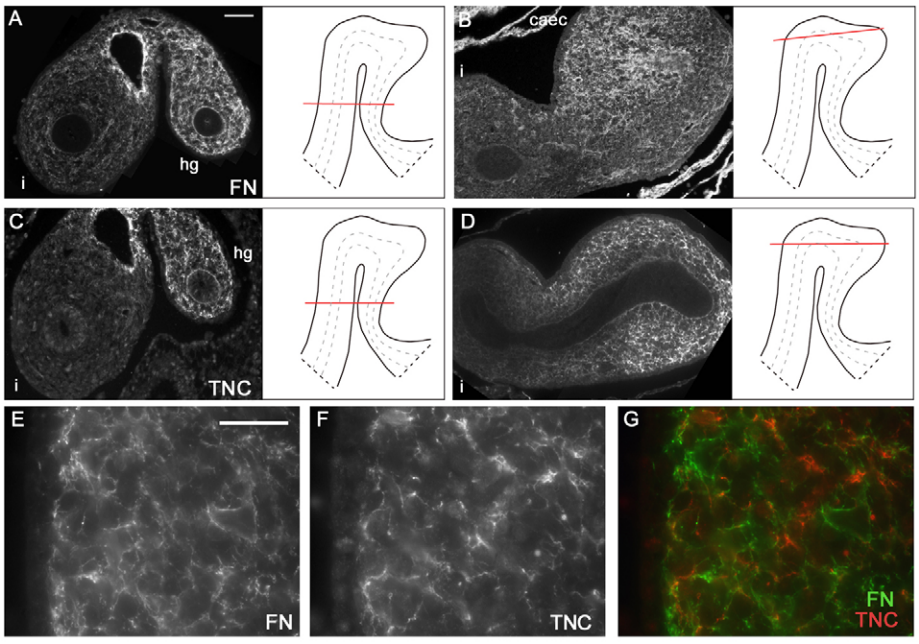

Fig. 5. Expression patterns of FN and TNC in the E11.5 gut. (**A-D**) Immunostaining for FN (A,B) and TNC (C,D) on control E11.5 mouse gut sections. Accompanying schematics indicate the plane of section (red line) relative to the epithelium (dashed line). (**E-G**) High-magnification images of FN (E) and TNC (F) double immunostaining (G) in the E11.5 proximal hindgut. i, ileum; hg, hindgut. Scale bars: 50 μm.

proteins in the E11.5 embryonic gut. We found no difference in the expression pattern of any of the analysed ECM proteins between control and mutant guts (data not shown). Thus, both control and mutant ENCCs encounter a TNC- and FN-rich mesenchyme when they reach the base of the caecum at E11.5, which differs from their matrix environment in the ileum.

Effects of TNC and FN on the migration of control and β1 integrin mutant ENCCs in gut explant cultures

The change in the matrix environment at the level of the caecum and proximal hindgut correlates both in time and space with the onset of the migration phenotype of *Itgb1*-null ENCCs, and with the pause followed by the transition from a chain-like mode of locomotion to a migration involving mostly isolated cells observed for control ENCCs (Druckenbrod and Epstein, 2005). The stimulatory effect of FN on cell adhesion and migration, in particular for NCCs, is well established (Rovasio et al., 1983; Duband et al., 1990), whereas TNC can have either a positive or negative effect on these processes depending on the cell type and context of analysis (Halfter et al., 1989; Riou et al., 1992; Chiquet-Ehrismann, 2004). We examined the effect of TNC and FN on the migration of control and mutant ENCCs in vitro. VN was used as the substratum of reference owing to (1) its equivalent presence in the ileum, caecum and hindgut mesenchyme (Fig. 4G,H), and (2) its capacity to engage αv integrins, including αvβ5, which is expressed by *Itgb1*-null ENCCs, at least in the ileum (Breau et al., 2006). Thus, VN was likely to serve as a permissive substratum for *Itgb1*-null ENCCs, allowing us to evaluate the effects of TNC and FN on ENCC migration from rings of E12.5 midguts. In this type of culture, not only ENCCs, but also epithelial cells and smooth muscle cells (SMCs), migrate out of the explants (see Fig. S2A in the supplementary material).

On VN, a large number of control ENCCs migrated and formed scattered networks after 48 hours (see Fig. S2Aa in the supplementary material). A similar distribution was observed on VN+TNC (see Fig. S2Ab in the supplementary material), although control ENCCs remained more grouped in this condition. Mutant ENCCs also migrated out of the explants on VN, confirming that VN is a useful substratum with which to analyse β1 integrin-independent (and likely αv integrin-dependent) migration, which remains functional in these cells (see Fig. S2Ad in the supplementary material). The β1 integrin-independent migration was strongly perturbed when TNC was present. After 48 hours, a few mutant ENCCs were found around the explants, but these formed compact aggregates (see Fig. S2Ae in the supplementary material). On VN+FN, the migration of control ENCCs was strongly enhanced as most of them were found beyond the SMC front (see Fig. S2Ac in the supplementary material). The mutant ENCCs, however, displayed similar distribution on the VN+FN substratum to that observed on VN alone (see Fig. S2Af in the supplementary material).

To better understand how TNC and FN influence ENCC behaviour in such cultures, we performed time-lapse imaging after 24 hours of culture. ENCCs can be identified by detection of YFP (not shown) or simply by their morphology and refringency (Fig. 6A,B; see Movies 5-10 in the supplementary material). On VN, control ENCCs had a spread morphology and interacted with both surrounding SMCs and the ECM. These two kinds of interactions, ENCC-SMC and ENCC-ECM, might act in synergy to promote optimal migration of ENCCs out of the explant (Fig. 6A; see Movie 5 in the supplementary material). Mutant ENCCs also migrated on, and interacted with, the VN (Fig. 6A; see Movie 6 in the supplementary material). On VN+TNC, control ENCCs were also able to directly interact with the substratum (Fig. 6A; see Movie 7 in the supplementary material). By contrast, most of the mutant ENCCs failed to interact with this substratum and in consequence were often found on the SMC layer, forming aggregates close to the explant (see Movie 8 in the supplementary material). When directly contacting the VN+TNC substratum, retraction events were frequently detected and the mutant ENCCs often displayed a round morphology (Fig. 6A); this effect was not observed in control cultures. In the presence of FN, the migration of control ENCCs was strongly enhanced, as most of them were well spread and moved beyond the SMC front onto the substratum itself (Fig. 6A; see Movie 9 in the supplementary material), which was not observed on VN alone. The mutant ENCCs, however, displayed behaviours on the VN+FN substratum similar to those observed on VN alone, remaining behind the SMC front and only rarely interacting with, and spreading directly onto, the matrix (Fig. 6A; see Movie 10 in the supplementary material).

We tracked ENCCs found in interaction with each substratum at the beginning of the time-lapse (Fig. 6B,C). TNC and FN had diametrically opposite effects on control ENCC migration, with a reduced speed of locomotion on VN+TNC and a greatly increased speed on VN+FN. The decreased persistence of movement observed for control ENCCs on VN+FN could result from the more dispersed and highly motile phenotype of these cells and their migration beyond the SMC layer (and its influence). In contrast to control ENCCs, mutant cells did not positively respond to FN in their migration, which clearly demonstrates that FN promotes ENCC migration through a β1 integrin-dependent mechanism. As in control cultures, the speed of mutant ENCCs was reduced in the presence of TNC. The increased persistence of mutant ENCCs on VN+TNC, which was not observed in controls, is likely to be due to their more passive migration on this substratum, keeping them in longer association with SMCs. Another way to quantify the effect of TNC on migration is to evaluate the percentage of ENCC clusters found in the outer zone of the culture after 48 hours (see Fig. S2 in the supplementary material). We found that mutant ENCCs seemed more sensitive than controls to the TNC effect (75% inhibition rate for the mutant, 30% for the control). The stronger effect of TNC on *Itgb1*-null ENCCs as obtained with this second quantification method is probably due to the fact that it took all ENCCs into account, even those that failed to interact with the substratum early on during the culture period.

In order to determine whether TNC and FN affect the migration and/or morphology of specific ENCC subpopulations, we carried out immunostainings on some of the explants after 48 hours of culture for SOX10, a transcription factor that is expressed by both glial cells and undifferentiated ENCC progenitors, for the pan-neuronal markers HuD and NF160 (ELAVL4 and NEFM – Mouse Genome Informatics) and for the glial marker B-FABP (FABP7). This allowed us to identify progenitors ($SOX10^+$ B-$FABP^-$ $NF160/HuD^-$), glial cells ($SOX10^+$ B-$FABP^+$ $NF160/HuD^-$) and neurons ($SOX10^-$ B-$FABP^-$ $NF160/HuD^+$). In all the conditions analysed, progenitors, neurons and glial cells were found in similar proportions (Fig. 7A), indicating that TNC and FN do not affect the migration of a particular cell type out of the explants. We then analysed the morphology of these cell types on the three different substrata. TNC had no obvious effect on control ENCC morphology (Fig. 7Ba,b,d,e). By contrast, mutant $SOX10^+$ cells (including both glial cells and progenitors), but not $NF160^+$ cells, exhibited a more compact morphology in the presence of TNC than on VN alone (Fig. 7Bg,h,j,k). In control cultures, $SOX10^+$

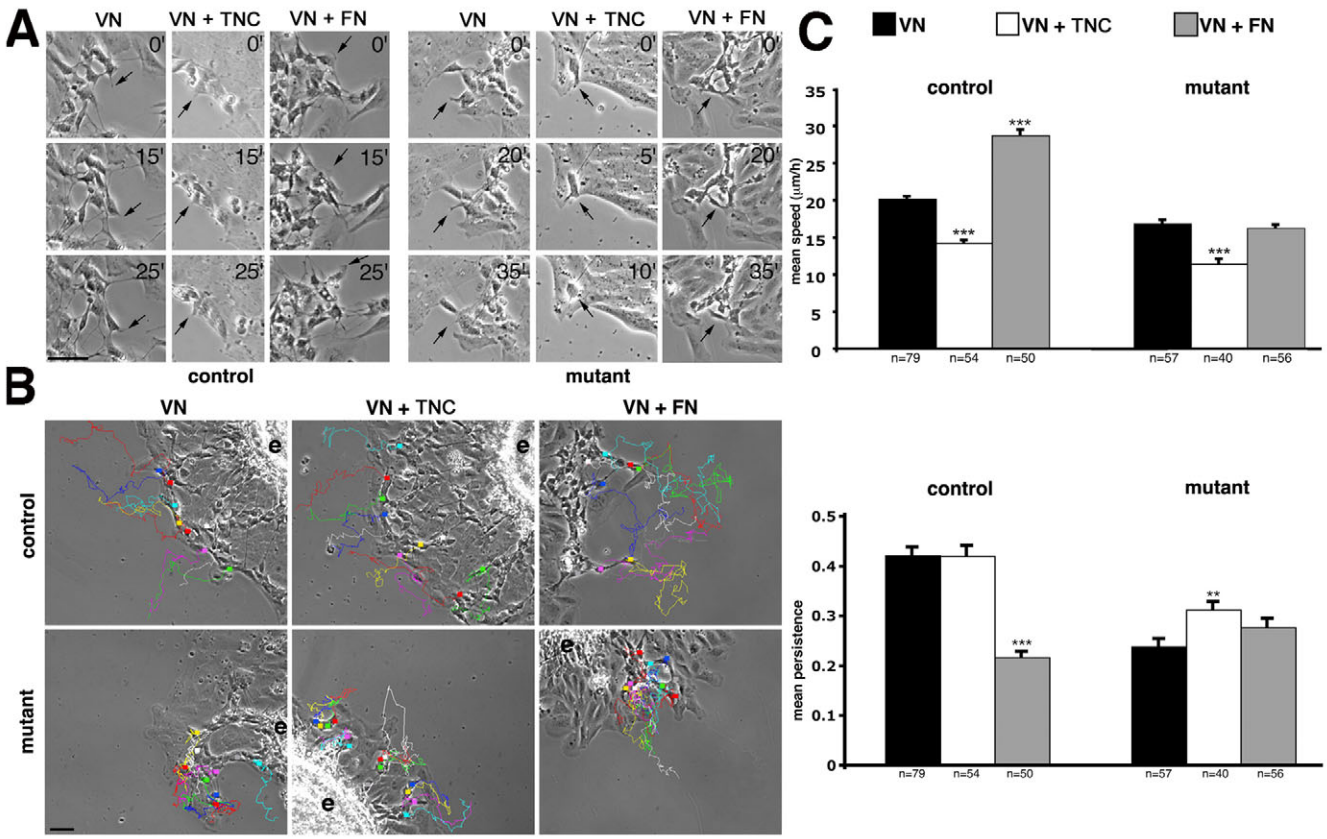

Fig. 6. Effects of TNC and FN on ENCC migration in gut explant cultures. (**A**) Images extracted from movies of mouse gut explant cultures after 24 hours, showing interactions between control and mutant ENCCs and the substratum. Arrows indicate direct contacts between ENCCs and the substratum and their evolution over time (minutes). (**B**) Phase-contrast images extracted at time 0 from movies of gut explant cultures on the three substrata. Coloured squares and lines indicate the initial positions and trajectories of tracked ENCCs, respectively. e, explant (for control on VN+FN, the explant is on the left, outside of the imaged field). (**C**) Mean speed and persistence of ENCC movements. The number of tracked cells is indicated beneath each column, with at least five different explants (obtained from five control and three mutant guts) analysed per condition. Error bars indicate s.e.m. $**P<0.01$, $***P<0.0001$, Student's *t*-test. Scale bars: 50 µm.

cells, but not NF160$^+$ cells, were more spread on the VN+FN substratum than on VN alone (Fig. 7Ba,c,d,f). However, this positive effect of FN on the spreading of SOX10$^+$ cells was not observed in the mutant (Fig. 7Bg,i,j,l). Thus, the spreading of *Itgb1*-null, but not control, SOX10$^+$ ENCCs seems to be prevented by TNC, whereas FN stimulates the spreading of control, but not mutant, SOX10$^+$ cells. Although the link between the morphology of SOX10$^+$ cells and the migration of the whole ENCC population out of the explants remains to be established, it is likely that both ECM components influence control and mutant ENCC migration through a specific effect on the migration of the SOX10$^+$ cell population.

Effects of TNC and FN on the adhesion and spreading of isolated control and β1 integrin mutant ENCCs in vitro

To further understand the role of TNC and FN in the adhesion properties of control and mutant ENCCs that reach the base of the caecum, we used an in vitro assay to quantify adhesion and spreading, bypassing interactions between ENCCs and SMCs. E12 midguts were dissociated and the resulting single-cell suspension was plated onto VN, VN+TNC or VN+FN. Adherent cells were analysed for ENCC marker expression. Results from B-FABP staining were ambiguous on such isolated cells (not shown), preventing the identification of glial cells within the SOX10$^+$ population. However, because only a small segment of the proximal midgut contains differentiated B-FABP$^+$ glial cells at E12 (Paratore et al., 2002; Young et al., 2003), the SOX10$^+$ population mostly consists of undifferentiated ENCC progenitors in our short-term cultures.

On VN alone, control and mutant cultures had similar proportions of adherent (round and spread) NF160$^+$ and SOX10$^+$ cells (Fig. 8A). The proportion of adherent SOX10$^+$ cells in mutant cultures was significantly lower on VN+TNC than on VN. The same tendency was observed in control cultures, although the reduction observed was not significant. These results suggest that TNC inhibits the adhesion of SOX10$^+$ progenitors on VN, with a greater inhibitory effect in the β1 integrin mutants. The proportion of adherent control SOX10$^+$ cells was significantly greater on VN+FN than on VN alone. By contrast, no difference was found in the adhesion potential of mutant SOX10$^+$ cells between VN and VN+FN plates. FN also had a strong positive effect on the percentage of spread (adherent cells exhibiting lamellipodia or membrane protrusions) control SOX10$^+$ cells, whereas no increase was detected for the mutant (Fig. 8B). These observations show that FN promotes the adhesion and spreading of SOX10$^+$ undifferentiated progenitors through a β1 integrin-dependent mechanism.

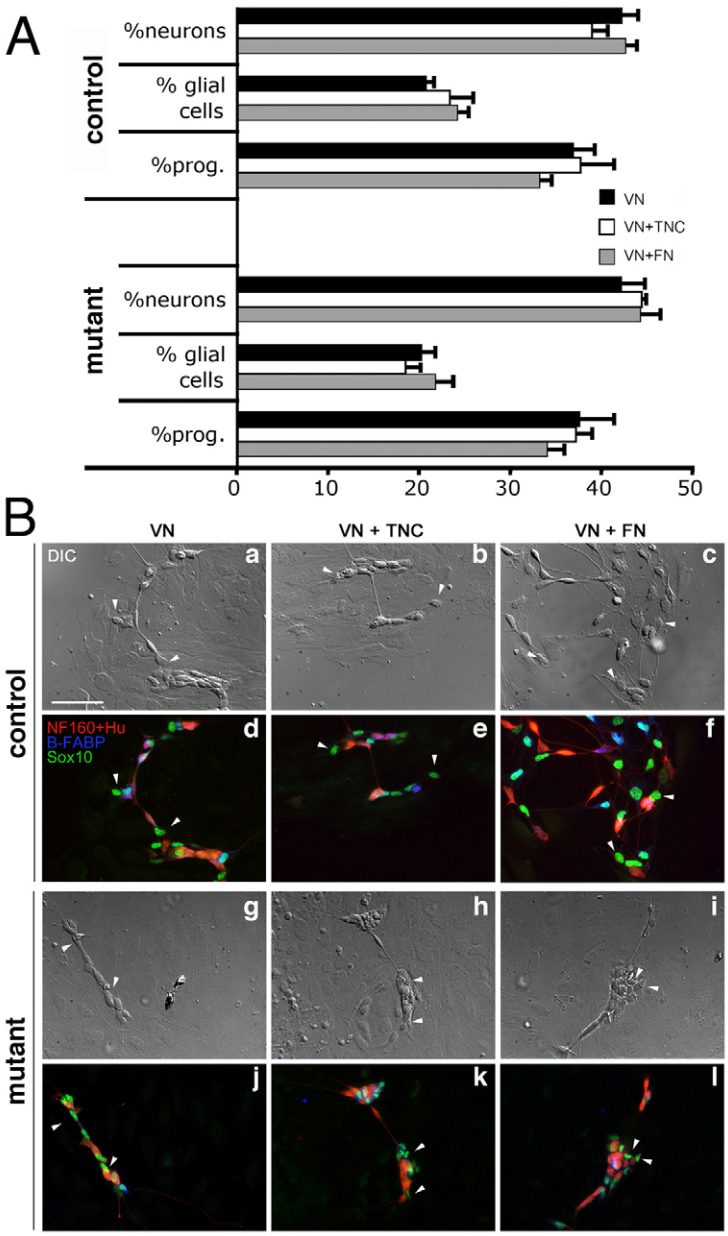

Fig. 7. Effects of TNC and FN on the migration and morphology of different ENCC subtypes in gut explant cultures. (**A**) The percentage of neurons, glial cells and undifferentiated progenitors (prog.) found among the control and mutant ENCC populations on the three substrata. (**Ba-l**) Representative DIC images (a-c,g-i) and triple immunostaining (d-f,j-l) for SOX10 (green), B-FABP (blue) and NF160/HuD (red) in control (a-f) and mutant (g-l) gut explants on the three substrata. On DIC images, ENCCs are easily distinguishable by their shape and higher refringency. The arrowheads indicate examples of progenitors. Scale bar: 50 μm.

These findings, together with the results obtained from our migration assay, show that the loss of the β1 integrins affects the response of ENCCs, in particular the response of SOX10$^+$ cells, to the effects of TNC and FN. Without β1 integrins, ENCCs are more sensitive to the inhibitory effect of TNC on adhesion, spreading and migration, and do not respond to the stimulatory effect of FN. Since the ENCCs that primarily invade the caecum in vivo are mostly SOX10$^+$ undifferentiated progenitors, the altered response of *Itgb1*-null SOX10$^+$ ENCCs to TNC and FN must account for the region-specific migration phenotype during caecum and hindgut colonisation.

DISCUSSION

We showed a migration defect of *Itgb1*-null ENCCs during the invasion of the caecum and proximal hindgut. This correlated with the localised high-level expression of TNC (a negative regulator of ENCC adhesion and migration) and FN (a positive regulator for control ENCC migration), within the mesenchyme of these regions. By contrast, the timing of midgut colonisation is unchanged in mutants. The extracellular environment in the midgut is therefore permissive for the migration of ENCCs lacking β1 integrins at their surface. In this region, the migration of these cells is likely to be mainly dependent on their interactions with surrounding SMCs or VN, interactions that are still functional in mutant ENCCs. Consistent with this notion, we found that TNC and FN were present at only very low levels in the midgut. β1 integrin-independent interactions between ENCCs and other ECM components present in the midgut wall might also play a role in the invasion of this portion of the gut.

The normal colonisation of ENCCs is arrested in mutants at the base of the caecum at E11.5. These cells subsequently invade the caecum and proximal hindgut by forming abnormal aggregates, suggesting that the interaction between ENCCs and their extracellular environment is impaired from the caecum onwards. We

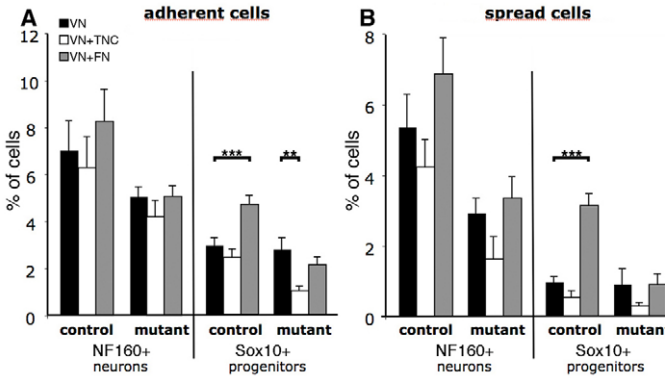

Fig. 8. Effects of TNC and FN on the adhesion and spreading of isolated ENCCs in vitro. Dissociated cells from control and mutant E12 mouse midguts were plated on surfaces coated with VN, VN+TN or VN+FN. The proportion of (**A**) adherent and (**B**) spread NF160$^+$ and SOX10$^+$ cells among the total population of adherent gut cells is shown. Control, *n*=6 guts; mutant, *n*=5. Error bars indicate s.e.m. ***P<0.005, **P<0.01, Mann-Whitney U-test.

showed that the E11.5 midgut and caecum/hindgut ECM share common components, including LN1, LNα5 and ColIV, which were found in the basal laminae, and VN, which was present in the pericellular spaces around epithelial and mesenchymal cells. By contrast, TNC and FN were found to be spatially regulated along the gut axis at this stage, with high levels of expression in the caecum and hindgut.

We compared the adhesion, morphology and migration of ENCCs on 2-D substrata that mimic the ECM of the midgut (VN alone) or caecum/hindgut (VN with TNC or FN). TNC is present during embryonic development and in adult remodelling tissues, such as in wounds and solid tumour stromal microenvironments. TNC has been found in the migratory pathways of NCCs in vivo (Tan et al., 1987; Mackie et al., 1988), and is necessary for the delamination of NCCs from the neural tube and their precocious migration in the chick (Tucker, 2001). During these processes, TNC is secreted by the NCCs themselves (Tucker and McKay, 1991). TNC promotes NCC migration in vitro (Halfter et al., 1989), but has also been shown to inhibit cell adhesion on various substrata, including FN (Chiquet-Ehrismann et al., 1988; Kiernan et al., 1996; Wenk et al., 2000; Midwood et al., 2004; Chiquet-Ehrismann and Tucker, 2004; Trebaul et al., 2007). Thus, the effect of TNC on cell adhesion and migration depends on the cell type or tissue and on the context of analysis. Furthermore, different isolated TNC recombinant domains have been found to act as negative or positive modulators of cell adhesion on FN (Saito et al., 2007). Here, we showed that TNC inhibits the migration of ENCCs and the adhesion of ENCCs on VN in vitro. Mutant ENCCs initiating a contact with TNC in vitro displayed a round morphology reminiscent of that of isolated ENCCs and ENCC clusters observed within the caecum and proximal hindgut regions.

To further assess the potential contribution of TNC to the in vivo migration phenotype in the mutant, we performed graft experiments to analyse the migration of control and mutant ENCCs coming from distal midgut segments into *Tnc*$^{+/-}$ hindgut segments (see Fig. S3 in the supplementary material). These segments contain a reduced amount of TNC but exhibit no change in the expression of other ECM components, including TNW (not shown). We previously showed in similar experiments using wild-type hindgut segments as recipients, that the distance travelled by mutant ENCCs in the hindgut is significantly reduced (by 34%) compared with controls (Breau et al., 2006). Here, we observed no significant difference in the distance travelled in *Tnc*$^{+/-}$ hindgut between control and mutant ENCCs. This suggests that a reduction in the amount of TNC present in the hindgut environment can at least partly rescue the migration defect of *Itgb1*-null ENCCs.

The effect of TNC on wild-type ENCCs in vivo remains unexplained. It is known that ENCCs pause at the base of the caecum for a few hours before invading it as solitary cells (Druckenbrod and Epstein, 2005). The inhibitory effect of TNC, which is strongly expressed in the caecum, could account for the temporary arrest in migration, which in turn might give the ENCCs time to integrate the complex array of signals available there [e.g. GDNF and EDN3 stimulation, other ECM-dependent signals such as that of FN, and repulsive signals such as those from semaphorin 3A and 3F (Anderson et al., 2007)] to change their fate or patterns of cell surface receptors and pursue their migration with a different mode of locomotion. One role of the caecum could be to delay the vagal NCC migration so that sacral NCCs (Burns and Le Douarin, 1998; Kapur, 2000) can occupy the most distal territory. Thus, TNC could be one of the players that modulate ENCC migration from the caecum onwards. Additional graft experiments using wild-type, *Tnc*$^{+/-}$ and *Tnc*$^{-/-}$ hindgut fragments as hosts, along with the analysis of gut colonisation in *Tnc*$^{-/-}$ mice, will be necessary to clarify the role of TNC in ENCC migration, but these experiments are beyond the scope of this study.

FN promotes cell adhesion and migration for most cell types, in particular for NCCs (Rovasio et al., 1983; Bronner-Fraser, 1986; Testaz et al., 1999; Testaz and Duband, 2001). Here, we showed that FN markedly improves the migration of control ENCCs and the adhesion and spreading of control SOX10$^+$ progenitors in a β1 integrin-dependent manner. Interactions between FN and β1 integrin may therefore promote the in vivo invasion of the caecum and proximal hindgut by ENCCs, and in particular by SOX10$^+$ undifferentiated progenitors. The absence of these interactions in mutants must contribute to the region-specific migration phenotype.

Sacral NCCs could also respond to TNC and FN when they enter the caudal hindgut. We detected slightly lower (but significant) levels of TNC in this region as compared with those in the proximal hindgut and caecum at E12.5 (not shown), but we did not check TNC levels at the stage of sacral colonisation (E13.5). X-Gal staining in the pelvic ganglia in mutants indicated that the *Itgb1*-null sacral NCCs reached the caudal extremity of the hindgut. However, sacral NCCs do not enter the hindgut in mutants (Breau et al., 2006). The presence of TNC and FN might have an effect on this process, as well as on the delayed invasion of the hindgut by wild-type sacral NCCs.

It remains to identify the repertoire of integrins expressed by ENCCs, and which integrins mediate the effects of TNC and FN. Given that *Itgb1*-null ENCCs are sensitive to the inhibitory effect of TNC, this effect must be mediated by non-β1 integrins, i.e. αv integrins, or other receptors yet to be discovered. Both αvβ3 and αvβ5 integrins are present in control and mutant ENCCs (Breau et al., 2006) and are good candidates for mediating the inhibitory effect of TNC. The stimulatory effect of FN on ENCC adhesion, spreading and migration is clearly β1 integrin-dependent. FN could act through interaction with α4β1 integrin, which is potentially present at the ENCC surface (Kruger et al., 2002; Breau et al., 2006) and is involved in trunk NCC migration on FN in vitro (Testaz et al., 1999; Testaz and Duband, 2001), but might also act through α5β1 integrin, which is also expressed by ENCCs (our unpublished data).

The different responses of NF160$^+$ neurons and SOX10$^+$ cells in our in vitro assays suggest a differential expression of integrins between the different ENCC lineages, making the situation even more complex. It is also likely that the integrin activation state at the ENCC surface changes over time. A recent study revealed that exposure to the caecum impairs the ability of ENCCs to migrate back towards an aneural midgut (Anderson et al., 2007). This could reflect a change in the adhesive properties of ENCCs when they enter the caecum, comprising, for example, a non-reversible switch in the expression/activation state of integrins.

Based on our observations, we propose the following hypothesis to explain the region-specific migration phenotype in β1 integrin mutants. Inhibition by TNC of ENCC adhesion and migration may be responsible for the arrest of ENCC migration at the base of the caecum in vivo, in both control and *Itgb1*-null cells. β1 integrins may be required for counteracting this inhibitory effect and for permitting further rostrocaudal migration through the FN-rich caecum and proximal hindgut ECM. Other mechanisms could also contribute to this localised migration phenotype. In particular, the EDN3/EDNRB and GDNF/GFRα/RET pathways could interact with β1 integrin adhesion and/or signalling within ENCCs to promote invasion of the caecum. EDN3/EDNRB signalling is only required between E11.5 and E12.5, corresponding exactly to the timing of caecum/proximal hindgut invasion (Shin et al., 1999; Woodward et al., 2000). Interestingly, TNC can interact with EDNRA and EDNRB signalling in different cancer cell lines (Ruiz et al., 2004; Lange et al., 2007), and thus could interact with the EDN3/EDNRB signalling pathway to regulate caecum invasion by ENCCs.

Acknowledgements

The anti-NF160 monoclonal antibody (2H3) was obtained from the Developmental Studies Hybridoma Bank, developed under the auspices of the NICHD and maintained by the Department of Biological Sciences, University of Iowa, Iowa City, IA 52242, USA. We thank V. Fraisier for help with imaging and computerised video microscopy; N. Bondurand and L. Stanchina for advice on embryonic gut dissociation; P. Simon Assmann, J.-L. Duband, T. Müller and M. Wegner for providing antibodies; M. Schachner for providing TNC-deficient mice; and W. A. Thomas for reading of the manuscript. This work was supported by the Centre National de la Recherche Scientifique, the Institut Curie and the Association pour la Recherche sur le Cancer (ARC) (grants 3737 and 4864). M.A.B. was supported by an AMN fellowship from the Ministère de l'Education Nationale, de l'Enseignement Supérieur et de la Recherche and an ARC fellowship.

Supplementary material

Supplementary material for this article is available at http://dev.biologists.org/cgi/content/full/136/16/2791/DC1

References

Anderson, R. B., Bergner, A. J., Taniguchi, M., Fujisawa, H., Forrai, A., Robb, L. and Young, H. M. (2007). Effects of different regions of the developing gut on the migration of enteric neural crest-derived cells: a role for Sema3A, but not Sema3F. *Dev. Biol.* **305**, 287-299.

Barlow, A., de Graaff, E. and Pachnis, V. (2003). Enteric nervous system progenitors are coordinately controlled by the G protein-coupled receptor EDNRB and the receptor tyrosine kinase RET. *Neuron* **40**, 905-916.

Beauvais-Jouneau, A., Delouvée, A., Craig, S. E., Humphries, M. J., Thiery, J. P. and Dufour, S. (1997). Direct role of the carboxy-terminal cell-binding domain of fibronectin in neural crest cell motility. *Exp. Cell Res.* **233**, 1-10.

Bolcato-Bellemin, A. L., Lefèbvre, O., Arnold, C., Sorokin, L., Miner, J. H., Kedinger, M. and Simon-Assmann, P. (2003). Laminin alpha5 chain is required for intestinal smooth muscle development. *Dev. Biol.* **260**, 376-390.

Breau, M. A., Pietri, T., Eder, O., Blanche, M., Brakebusch, C., Fassler, R., Thiery, J. P. and Dufour, S. (2006). Lack of beta1 integrins in enteric neural crest cells leads to a Hirschsprung-like phenotype. *Development* **133**, 1725-1734.

Bronner-Fraser, M. (1986). An antibody to a receptor for fibronectin and laminin perturbs cranial neural crest development in vivo. *Dev. Biol.* **117**, 528-536.

Burns, A. J. and Douarin, N. M. (1998). The sacral neural crest contributes neurons and glia to the post-umbilical gut: spatiotemporal analysis of the development of the enteric nervous system. *Development* **125**, 4335-4347.

Chalazonitis, A., D'Autreaux, F., Guha, U., Pham, T. D., Faure, C., Chen, J. J., Roman, D., Kan, L., Rothman, T. P., Kessler, J. A. et al. (2004). Bone morphogenetic protein-2 and -4 limit the number of enteric neurons but promote development of a TrkC-expressing neurotrophin-3-dependent subset. *J. Neurosci.* **24**, 4266-4282.

Chiquet-Ehrismann, R. (2004). Tenascins. *Int. J. Biochem. Cell Biol.* **36**, 986-990.

Chiquet-Ehrismann, R. and Tucker, R. P. (2004). Connective tissues: signalling by tenascins. *Int. J. Biochem. Cell Biol.* **36**, 1085-1089.

Chiquet-Ehrismann, R., Kalla, P., Pearson, C. A., Beck, K. and Chiquet, M. (1988). Tenascin interferes with fibronectin action. *Cell* **53**, 383-390.

Druckenbrod, N. R. and Epstein, M. L. (2005). The pattern of neural crest advance in the cecum and colon. *Dev. Biol.* **287**, 125-133.

Druckenbrod, N. R. and Epstein, M. L. (2007). Behavior of enteric neural crest-derived cells varies with respect to the migratory wavefront. *Dev. Dyn.* **236**, 84-92.

Duband, J. L., Dufour, S. and Thiery, J. P. (1990). The instructive role of fibronectins in cell migrations. *Ann. New York Acad. Sci.* **588**, 273-280.

Evers, M. R., Salmen, B., Bukalo, O., Rollenhagen, A., Bosl, M. R., Morellini, F., Bartsch, U., Dityatev, A. and Schachner, M. (2002). Impairment of L-type Ca^{2+} channel-dependent forms of hippocampal synaptic plasticity in mice deficient in the extracellular matrix glycoprotein tenascin-C. *J. Neurosci.* **22**, 7177-7194.

Fujimoto, T., Hata, J., Yokoyama, S. and Mitomi, T. (1989). A study of the extracellular matrix protein as the migration pathway of neural crest cells in the gut: analysis in human embryos with special reference to the pathogenesis of Hirschsprung's disease. *J. Pediatr. Surg.* **24**, 550-556.

Halfter, W., Chiquet-Ehrismann, R. and Tucker, R. P. (1989). The effect of tenascin and embryonic basal lamina on the behavior and morphology of neural crest cells in vitro. *Dev. Biol.* **132**, 14-25.

Hynes, R. O. (2002). Integrins: bidirectional, allosteric signaling machines. *Cell* **110**, 673-687.

Kapur, R. P. (2000). Colonization of the murine hindgut by sacral crest-derived neural precursors: experimental support for an evolutionarily conserved model. *Dev. Biol.* **227**, 146-155.

Kaufman, M. H. (1995). *The Atlas of Mouse Development*, 2nd edn. London: Academic Press.

Kerr, R. S. and Newgreen, D. F. (1997). Isolation and characterization of chondroitin sulfate proteoglycans from embryonic quail that influence neural crest cell behavior. *Dev. Biol.* **192**, 108-124.

Kiernan, B. W., Gotz, B., Faissner, A. and ffrench-Constant, C. (1996). Tenascin-C inhibits oligodendrocyte precursor cell migration by both adhesion-dependent and adhesion-independent mechanisms. *Mol. Cell. Neurosci.* **7**, 322-335.

Kruger, G. M., Mosher, J. T., Bixby, S., Joseph, N., Iwashita, T. and Morrison, S. J. (2002). Neural crest stem cells persist in the adult gut but undergo changes in self-renewal, neuronal subtype potential, and factor responsiveness. *Neuron* **35**, 657-669.

Kurtz, A., Zimmer, A., Schnutgen, F., Bruning, G., Spener, F. and Muller, T. (1994). The expression pattern of a novel gene encoding brain-fatty acid binding protein correlates with neuronal and glial cell development. *Development* **120**, 2637-2649.

Lange, K., Kammerer, M., Hegi, M. E., Grotegut, S., Dittmann, A., Huang, W., Fluri, E., Yip, G. W., Gotte, M., Ruiz, C. et al. (2007). Endothelin receptor type B counteracts tenascin-C-induced endothelin receptor type A-dependent focal adhesion and actin stress fiber disorganization. *Cancer Res.* **67**, 6163-6173.

Larsen, M., Artym, V. V., Green, J. A. and Yamada, K. M. (2006). The matrix reorganized: extracellular matrix remodeling and integrin signaling. *Curr. Opin. Cell Biol.* **18**, 463-471.

Lefèbvre, O., Sorokin, L., Kedinger, M. and Simon-Assmann, P. (1999). Developmental expression and cellular origin of the laminin alpha2, alpha4, and alpha5 chains in the intestine. *Dev. Biol.* **210**, 135-150.

Leibl, M. A., Ota, T., Woodward, M. N., Kenny, S. E., Lloyd, D. A., Vaillant, C. R. and Edgar, D. H. (1999). Expression of endothelin 3 by mesenchymal cells of embryonic mouse caecum. *Gut* **44**, 246-252.

Mackie, E. J., Tucker, R. P., Halfter, W., Chiquet-Ehrismann, R. and Epperlein, H. H. (1988). The distribution of tenascin coincides with pathways of neural crest cell migration. *Development* **102**, 237-250.

Maka, M., Stolt, C. C. and Wegner, M. (2005). Identification of Sox8 as a modifier gene in a mouse model of Hirschsprung disease reveals underlying molecular defect. *Dev. Biol.* **277**, 155-169.

Marusich, M. F., Furneaux, H. M., Henion, P. D. and Weston, J. A. (1994). Hu neuronal proteins are expressed in proliferating neurogenic cells. *J. Neurobiol.* **25**, 143-155.

Midwood, K. S., Valenick, L. V., Hsia, H. C. and Schwarzbauer, J. E. (2004). Coregulation of fibronectin signaling and matrix contraction by tenascin-C and syndecan-4. *Mol. Biol. Cell* **15**, 5670-5677.

Natarajan, D., Marcos-Gutierrez, C., Pachnis, V. and de Graaff, E. (2002). Requirement of signalling by receptor tyrosine kinase RET for the directed

migration of enteric nervous system progenitor cells during mammalian embryogenesis. *Development* **129**, 5151-5160.
Neugebauer, K. M., Emmett, C. J., Venstrom, K. A. and Reichardt, L. F. (1991). Vitronectin and thrombospondin promote retinal neurite outgrowth: developmental regulation and role of integrins. *Neuron* **6**, 345-358.
Newgreen, D. F. and Hartley, L. (1995). Extracellular matrix and adhesive molecules in the early development of the gut and its innervation in normal and spotting lethal rat embryos. *Acta Anat. (Basel)* **154**, 243-260.
Paratore, C., Eichenberger, C., Suter, U. and Sommer, L. (2002). Sox10 haploinsufficiency affects maintenance of progenitor cells in a mouse model of Hirschsprung disease. *Hum. Mol. Genet.* **11**, 3075-3085.
Perris, R., Perissinotto, D., Pettway, Z., Bronner-Fraser, M., Morgelin, M. and Kimata, K. (1996). Inhibitory effects of PG-H/aggrecan and PG-M/versican on avian neural crest cell migration. *FASEB J.* **10**, 293-301.
Pietri, T., Eder, O., Blanche, M., Thiery, J. P. and Dufour, S. (2003). The human tissue plasminogen activator-Cre mouse: a new tool for targeting specifically neural crest cells and their derivatives in vivo. *Dev. Biol.* **259**, 176-187.
Potocnik, A. J., Brakebusch, C. and Fassler, R. (2000). Fetal and adult hematopoietic stem cells require beta1 integrin function for colonizing fetal liver, spleen, and bone marrow. *Immunity* **12**, 653-663.
Riou, J. F., Umbhauer, M., Shi, D. L. and Boucaut, J. C. (1992). Tenascin: a potential modulator of cell-extracellular matrix interactions during vertebrate embryogenesis. *Biol. Cell* **75**, 1-9.
Rovasio, R. A., Delouvee, A., Yamada, K. M., Timpl, R. and Thiery, J. P. (1983). Neural crest cell migration: requirements for exogenous fibronectin and high cell density. *J. Cell Biol.* **96**, 462-473.
Ruiz, C., Huang, W., Hegi, M. E., Lange, K., Hamou, M. F., Fluri, E., Oakeley, E. J., Chiquet-Ehrismann, R. and Orend, G. (2004). Growth promoting signaling by tenascin-C [corrected]. *Cancer Res.* **64**, 7377-7385.
Saito, Y., Imazeki, H., Miura, S., Yoshimura, T., Okutsu, H., Harada, Y., Ohwaki, T., Nagao, O., Kamiya, S., Hayashi, R. et al. (2007). A peptide derived from tenascin-C induces beta1 integrin activation through syndecan-4. *J. Biol. Chem.* **282**, 34929-34937.
Scherberich, A., Tucker, R. P., Samandari, E., Brown-Luedi, M., Martin, D. and Chiquet-Ehrismann, R. (2004). Murine tenascin-W: a novel mammalian tenascin expressed in kidney and at sites of bone and smooth muscle development. *J. Cell Sci.* **117**, 571-581.
Shin, M. K., Levorse, J. M., Ingram, R. S. and Tilghman, S. M. (1999). The temporal requirement for endothelin receptor-B signalling during neural crest development. *Nature* **402**, 496-501.
Simon-Assmann, P., Kedinger, M., De Arcangelis, A., Rousseau, V. and Simo, P. (1995). Extracellular matrix components in intestinal development. *Experientia* **51**, 883-900.
Sorokin, L. M., Pausch, F., Durbeej, M. and Ekblom, P. (1997). Differential expression of five laminin alpha (1-5) chains in developing and adult mouse kidney. *Dev. Dyn.* **210**, 446-462.
Srinivas, S., Watanabe, T., Lin, C. S., William, C. M., Tanabe, Y., Jessell, T. M. and Costantini, F. (2001). Cre reporter strains produced by targeted insertion of EYFP and ECFP into the ROSA26 locus. *BMC Dev. Biol.* **1**, 4.
Tan, S. S., Crossin, K. L., Hoffman, S. and Edelman, G. M. (1987). Asymmetric expression in somites of cytotactin and its proteoglycan ligand is correlated with neural crest cell distribution. *Proc. Natl. Acad. Sci. USA* **84**, 7977-7981.
Testaz, S. and Duband, J. L. (2001). Central role of the alpha4beta1 integrin in the coordination of avian truncal neural crest cell adhesion, migration, and survival. *Dev. Dyn.* **222**, 127-140.
Testaz, S., Delannet, M. and Duband, J. (1999). Adhesion and migration of avian neural crest cells on fibronectin require the cooperating activities of multiple integrins of the (beta)1 and (beta)3 families. *J. Cell Sci.* **112**, 4715-4728.
Trebaul, A., Chan, E. K. and Midwood, K. S. (2007). Regulation of fibroblast migration by tenascin-C. *Biochem. Soc. Trans.* **35**, 695-697.
Tucker, R. P. (2001). Abnormal neural crest cell migration after the in vivo knockdown of tenascin-C expression with morpholino antisense oligonucleotides. *Dev. Dyn.* **222**, 115-119.
Tucker, R. P. and McKay, S. E. (1991). The expression of tenascin by neural crest cells and glia. *Development* **112**, 1031-1039.
Wenk, M. B., Midwood, K. S. and Schwarzbauer, J. E. (2000). Tenascin-C suppresses Rho activation. *J. Cell Biol.* **150**, 913-920.
Woodward, M. N., Kenny, S. E., Vaillant, C., Lloyd, D. A. and Edgar, D. H. (2000). Time-dependent effects of endothelin-3 on enteric nervous system development in an organ culture model of Hirschsprung's disease. *J. Pediatr. Surg.* **35**, 25-29.
Young, H. M. and Newgreen, D. (2001). Enteric neural-crest derived cells: origin, identification, migration, and differentiation. *Anat. Rec.* **262**, 1-15.
Young, H. M., Hearn, C. J., Farlie, P. G., Canty, A. J., Thomas, P. Q. and Newgreen, D. F. (2001). GDNF is a chemoattractant for enteric neural cells. *Dev. Biol.* **229**, 503-516.
Young, H. M., Bergner, A. J. and Muller, T. (2003). Acquisition of neuronal and glial markers by neural crest-derived cells in the mouse intestine. *J. Comp. Neurol.* **456**, 1-11.
Young, H. M., Bergner, A. J., Anderson, R. B., Enomoto, H., Milbrandt, J., Newgreen, D. F. and Whitington, P. M. (2004). Dynamics of neural crest-derived cell migration in the embryonic mouse gut. *Dev. Biol.* **270**, 455-473.